Compact Plasma Device for PWI Studies

Shuichi TAKAMURA[1], Takayuki TSUJIKAWA[1], Yuji TOMIDA[1], Kengo SUZUKI[1], Takaaki MINAGAWA[1], Takanori MIYAMOTO[1] and Noriyasu OHNO[2]

1 Department of Electrical Engineering, Faculty of Engineering, Aichi Institute of Technology, Toyota 470-0392, Japan

2 Department of Energy Engineering and Science, Graduate School of Engineering, Nagoya University, Nagoya 464-8603, Japan

(Received: 22 October 2009 / Accepted: 20 March 2010)

Material selection for the first wall and divertor plate is essential to ensure a stable sustainment of tokamak plasma confinement and burning in ITER and DEMO. Tungsten is one of the most promising candidates. However, the surface damage due to helium irradiation is a serious concern to be overcome. Compact plasma device for such PWI (Plasma-Wall Interactions) studies is helpful to investigate, for example, how to avoid the helium damage of tungsten surface. In this paper the qualification of new plasma device for PWI is introduced, and the preliminary data of the effect of He irradiation on tungsten surface are shown.

Keywords: high–density plasma, plasma-wall interaction, tungsten, plasma-facing component, bubble and hole, nano-structure, ion bombardment

1. Introduction

Towards ITER and DEMO, material selection for the first wall and divertor plate inside the reactor is essential to ensure a stable sustainment of tokamak plasma confinement and nuclear burning since the steady as well as transient heat load and particle flux are enormous and critical in terms of thermal resistance of plasma-facing component [1, 2].

Tungsten seems to be one of the most promising candidates owing to a high melting temperature, a low sputtering yield and a relatively small tritium inventory. However, we have neither much experience in the environment of high power condition [3], nor the sufficient characterization as the first wall material. For example, the bubbles and holes formation at high surface temperature [4] and the arborescent nano-structure at relatively low surface temperature are the typical morphology of damaged surface which has a weak thermal resistance in terms of impurity release by surface melting due to lost thermal conduction to the deep bulk [5 – 8].

We need some test facilities to investigate the material properties for tungsten wall from various points of view in the reactor relevant condition. Compact plasma device for such PWI studies is very helpful to investigate, for example, how to avoid the helium damage of tungsten surface in terms of tungsten fabrication process such as ultra-fine grain tungsten [9], and thin carbon film deposition on the tungsten surface.

In the present paper the qualification of new plasma device for PWI studies is introduced and some preliminary data concerning the effect of helium plasma irradiation on powder metallurgy tungsten surface are shown.

author's e-mail: takamura@aitech.ac.jp

2. Compact Plasma Device

2.1 Device specification

In order to investigate PWI, especially helium effect on tungsten surface, we need to have a sufficient ion flux and heat load to the target relevant to those in fusion machines. The ion flux of more than 10^{22} $(m^2s)^{-1}$, hopefully 10^{23} $(m^2s)^{-1}$, and the heat load of more than 1 MW/m^2, hopefully 10 MW/m^2. Therefore, the plasma density is at least higher than 1 x 10^{18} m^{-3} and the electron temperature would be higher than 5 eV.

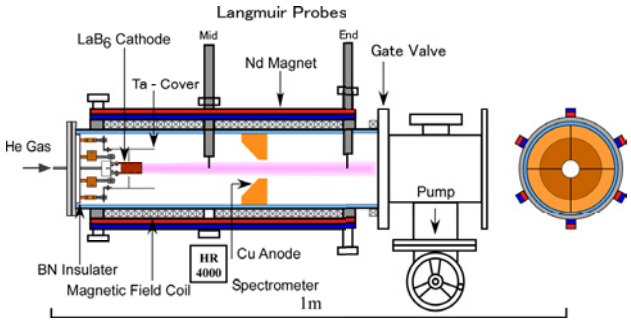

Fig.1 Schematic view of the device AIT-PID.

Our device called AIT-PID (Aichi Institute of Technology – Plasma Irradiation Device) has a machine structure shown in Fig.1, which is equipped with three pairs of neodymium permanent magnet bars composing multi-cusp (poloidal mode number: 3) magnetic configuration and a solenoidal winding underneath the magnets producing a weak axial magnetic field. Figure 2 shows the distributions of vertical magnetic field intensity obtained by both experiment using gauss meter and

numerical analysis. The agreement between these two is quite good. We have magnetic-free zone on the axis, through which the produced plasma may path in the axial direction. At the end of this zone, the LaB_6 cylindrical cathode with the diameter of 20 mm is located, while the target would be put at the opposite end. For the gas discharge control the weak axial magnetic field is also generated. The working range of this B_z is a few tens Gauss. We note that the solenoidal winding is set inside the permanent magnet. Otherwise, the axial field is not generated inside the vacuum chamber due to the short circuit of magnetic field line through the permanent magnet.

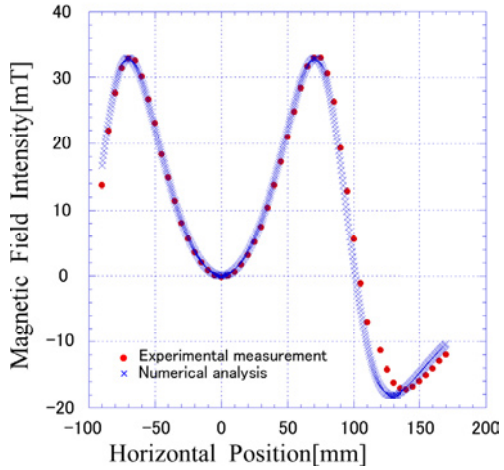

Fig.2 Comparison of horizontal profile of vertical magnetic field intensities between numerical analysis and measurements with gauss meter.

Usually, a strong magnetic field has been employed in linear plasma devices [5-8, 10-13] for the radial confinement of produced plasma. The consumed electric power for the magnetic coils is sometimes enormous. Not only a contribution to energy saving, but also a favorable effect on the maintenance of direct heated LaB_6 ceramic cathode have been obtained, that is, a very weak Lorenz stress on LaB_6 fragile ceramics coil due to the weak or zero magnetic field is ensured.

The grounded anode made of copper is set at the middle of the machine with a hole of diameter of 35 mm at the center, which produces the gas compression at the discharge region by a factor of about 2 due to narrow gas channel. The gas compression is also enhanced by the plasma plugging although it is modest a few % at the discharge current of 20 A. A higher plugging would be foreseen at higher discharge current. The present power supply can provide 50 A with the voltage up to 160 V.

The heat removal is very important in such a high-power and compact plasma device. The main discharge chamber has a double wall structure through which a cooling water circulation ensures the efficient heat removal. The water supply of 4.5 L/min with a temperature rise of 5 degree C carries out 70 % of the power injected into the device, discharge and cathode heating power at the level of discharge current of 20 A.

2.2 Measurement of plasma parameter

2.2.1 Plasma diagnostic equipment

As shown in Fig.1 a motor-driven scanning probe system is employed for the Langmuir probe diagnostics. It moves horizontally beyond the chamber center and is connected to A-D converter driven by PC to have digital data. The scanning speed is 0.51 cm/s and a series of triangle voltage (+50 to -100 V) is fed to the tungsten probe tip (0.8 mm in diameter and 2.3 mm in length) so that the I-V characteristics are obtained every 0.51 mm.

Another set of Langmuir probe is inserted from the end flange opposite to the cathode location. It is set just behind the anode hole. It is also used for the target holder of tungsten plate.

Figure 1 also shows the location of spectroscopic measurement. The quarts vacuum window may transmit the light emission from ultraviolet through infrared range (300 ~ 800 nm) using fiber optics and spectrometer (Ocean Optics Inc., HR-4000).

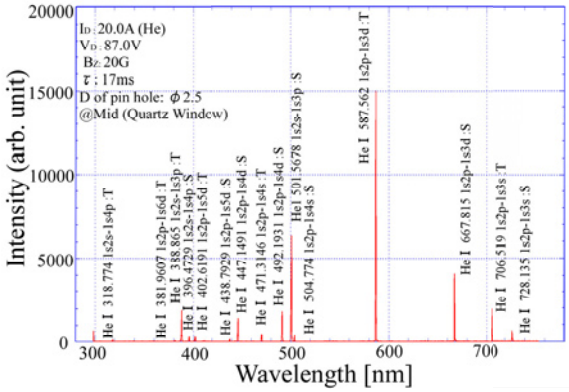

Fig.3 Light emission spectrum from He discharge plasma from ultraviolet through near-infrared lines.

2.2.2 Dependence of discharge current

We concentrate on the helium gas discharge although the argon gas is much easier for discharge to have high density plasmas. The helium gas flow rate is 60 ~ 70 sccm to have substantial discharge current with a modest discharge voltage less than 100 V. The discharge voltage of 100 V is not a critical figure, but we must be careful to minimize the sputtering of cathode-supporting material, mainly molybdenum and also LaB_6 itself due to helium ion bombardment.

As a first step the 20 A discharge plasma in steady state has been studied because the plasma density reaches to 10^{18} m^{-3}. An emission spectrum from pure He plasma has been obtained like in Fig.3. Figure 4 shows the spatial profile of ion saturation current, taking the discharge current I_D as a parameter. It increases roughly proportional to I_D.

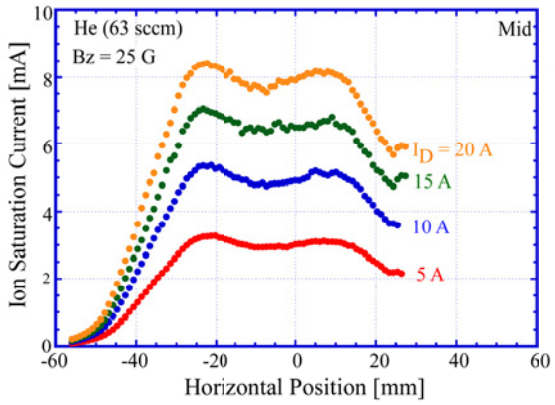

Fig.4 Horizontal profiles of ion saturation current, taking the discharge current I_D as a parameter.

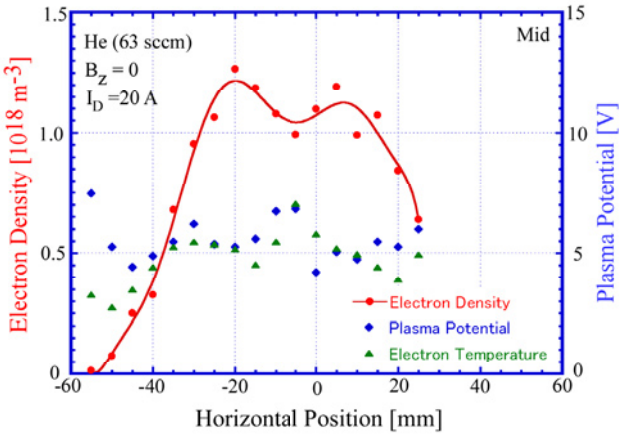

Fig.5 Horizontal profiles of electron density, temperature and plasma potential at the discharge current I_D of 20 A.

The spatial distributions of plasma density, electron temperature and plasma potential are shown in Fig.5, indicating the plasma potential is positively around 5 V with respect to the grounded chamber. The electron temperature is around 5 eV, corresponding to the bulk component. The probe *I-V* characteristics shown in Fig.6 reveal an energetic tail which is common over the whole discharge area. It seems to suggest a good confinement of high energy electrons in such a multi-cusp magnetic configuration. The presence of energetic electrons is preferable from the view point of plasma heat flux to the target since the effective electron temperature is higher than the value of bulk electrons.

The discharge current dependence of plasma parameter is shown in Fig.7 which indicates that the plasma density increases almost proportionally to I_D. The present power supply may provide the I_D up to 60 A.

2.2.3 Effect of axial magnetic field

It is not so clear at the moment what kind of role the axial magnetic field plays. However, it would be a control knob for obtaining stable and efficient discharge. The magnetic field intensity of a few tens gauss still gives relatively small Larmor radii of electrons, but comparable to the cathode diameter or the anode hole so that the discharge current path may either cross the magnetic field line or not influenced by the presence of axial magnetic field.

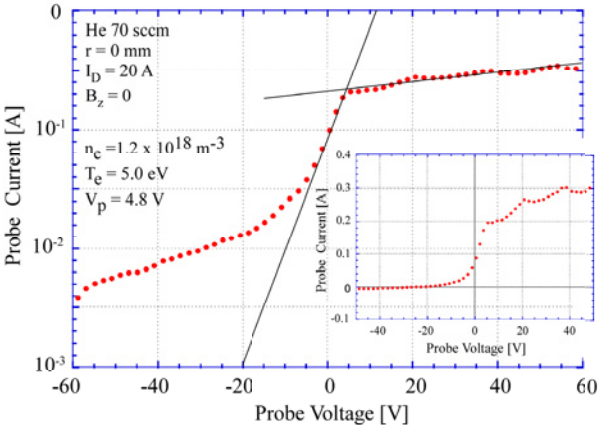

Fig.6 Logarithmic plot of electron current collected with a probe as a function of applied voltage.

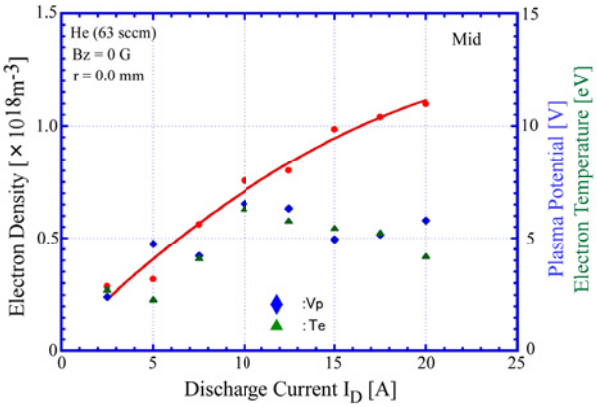

Fig.7 Dependence of the plasma parameters on the discharge current.

Figure 8 gives the horizontal distribution of ion saturation current, taking the coil current for B_z. Therefore, it seems that B_z gives favorable effects on the plasma parameter towards high density and high heat flux plasma generation.

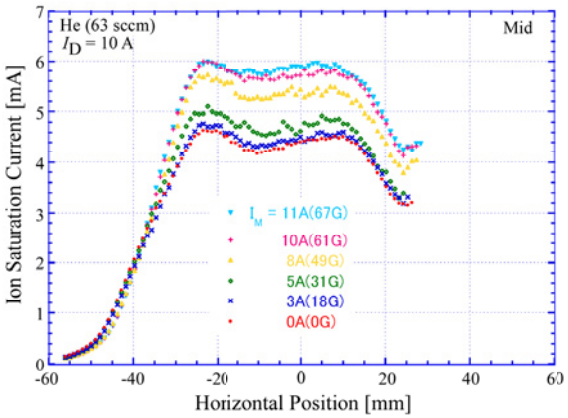

Fig.8 Horizontal profiles of ion saturation current, taking the intensity of axial magnetic field as a parameter.

The discharge voltage is drawn as a function of B_z in Fig.9, indicating an optimum coil current for I_D of 20 A would be 3 ~8 A corresponding to 18 ~ 49 gauss because we would like to minimize the discharge voltage without changing the plasma parameter. Rather, we have even some improvement of them, not shown here.

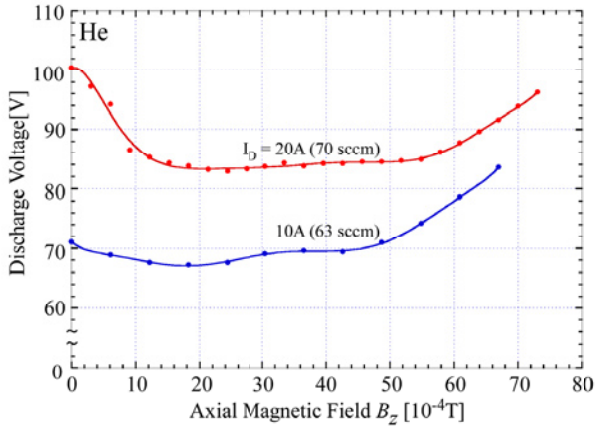

Fig.9 Dependence of the discharge voltage on the axial magnetic field for two different fixed discharge current I_D = 10 and 20 A.

3. Preliminary Trial of PWI

The high density helium plasma has been obtained with a good radial confinement using the multi-cusp field associated by a weak axial magnetic field. Preliminary trial of helium ion irradiation on the powder metallurgy tungsten has been performed in order to check the effectiveness of AIT-PID for the test facility of plasma-facing component. The tungsten target plate (15 x 15 mm^2) was inserted into the central position of AIT-PID at the same axial location as the scanning probe, but at the poloidally different port. The ion flux density is around 1 x 10^{22} $(m^2s)^{-1}$ and the ion fluence is 5 x 10^{25} m^{-2}.

Figure 10 shows some typical FE-SEM (Field Emission Scanning Electron-Microscope) images of tungsten surface with a surface temperature (1100 K ~ 1300 K) while irradiation, obtained under a floating condition. The ion bombarding energy is about 50 eV. We can distinguish arborescent nanostructure on the damaged surface with a black color [5-8].

On the other hand, by biasing the target towards the plasma potential, we can increase the surface temperature up to around 1600 K. In this case the ion bombarding energy is reduced 25 ~ 30 eV. The obtained surface morphology is shown in Fig.11, which is quite different from those shown in Fig.10. The bubbles and holes are created [4], but the size of them is not as large as 1 micron as observed before, but by an order of magnitude smaller. It means an initial stage of the development of bubbles and holes. These have never been reported before.

4. Conclusion

The high heat flux plasma has been generated with a new linear plasma device AIT-PID which is characterized by a power-saving employment of permanent magnet instead of solenoidal magnetic field coil for the plasma confinement in the radial direction. The directly heated LaB_6 cathode for d.c. discharge is located along the central null line of multi-cusp magnetic field configuration so that the stress-free due to Lorentz force ensures a long-life operation. It is found that high energetic electrons are confined well probably owing to multi-cusp mirror configuration, which benefits an increase in plasma heat flux to the target. A weak axial magnetic field generated with a solenoidal coil underneath a series of permanent magnets can be used as a control knob for obtaining optimum discharge, for example, a reduction of discharge voltage, keeping the discharge current and the plasma parameters almost constant.

At the moment we have succeeded in the discharge current of 20 A while the plasma density exceeds 1 x 10^{18} m^{-3} with a substantial effective electron temperature of more than 5 eV. The discharge current may be increased with a careful observation of the heat flux on the inner wall surface of the vacuum vessel.

Preliminary experiments on PWI have been tried successfully, especially He plasma irradiation on tungsten surface, clarifying an initial formation stage of macroscopic bubbles and holes at high temperature and an arborescent nano-structure at lower surface temperature.

Acknowledgement

This work was supported by a Grant-in-Aid for Scientific Research (B) (20360414) from JSPS.

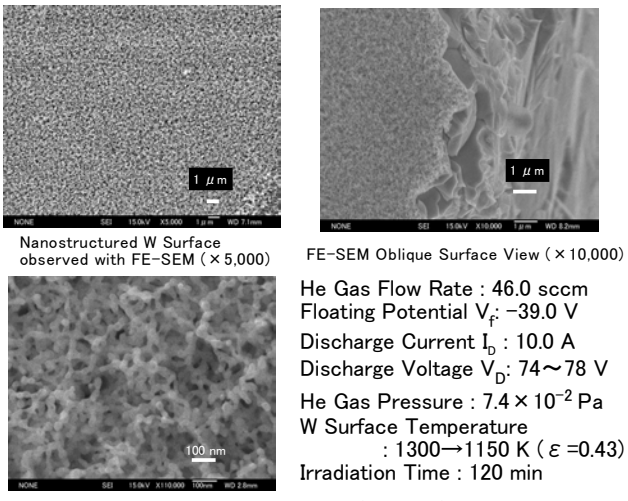

Fig.10 FE-SEM photos of arborescent nanostructure on the tungsten surface at relatively low surface temperature.

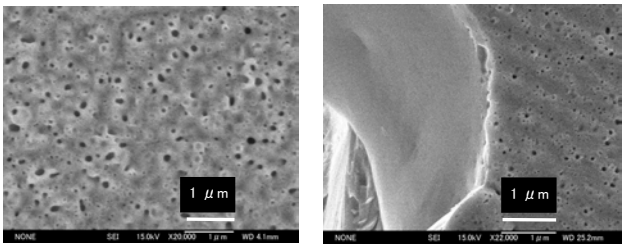

FE-SEM Surface Image (×20,000) FE-SEM Oblique Surface View (×22,000)

He Gas Flow Rate : 50 sccm
He Gas Pressure : 7.9×10^{-2} Pa
Discharge Current I_D : 20.0 A
Discharge Voltage V_D : 87～88 V
Bias Voltage V_B: −20V (Floating Potential V_f : −42 V)
Bias Current I_B: 600 mA
W Surface Temperature : 1700～1730 K (ε = 0.43)
Irradiation Time : 90 min

Fig.11 FE-SEM photos of small bubbles and holes on the tungsten surface at high surface temperature.

[1] A. Loarte, B. Lipschultz, A.S. Kukushkin et al., Nucl. Fusion **47**, S203 (2007).
[2] ITER Physics Expert Group on Divertor, ITER Physics Expert Group on Divertor Modelling and Database, and ITER Physics Basis Editors, Nucl. Fusion **39**, 2391 (1999).
[3] O. Gruber, A.C.C. Sips, R. Dux, T. Eich, J.C. Fuchs et al., Nucl. Fusion **49**, 115014 (2009).
[4] M.Y. Ye, S. Takamura and N. Ohno, J. Nucl. Mater. **241-243**, 1243 (1997).
[5] S. Takamura and N. Ohno, Plasma Fusion Res. **1**, 051 (2006).
[6] S. Kajita, S. Takamura and N. Ohno, Nucl. Fusion **49**, 032002 (2009).
[7] M.J. Baldwin, R.P. Doerner, D. Nishijima, K. Tokunaga and Y. Ueda, J. Nucl. Mater. **390-391**, 886 (2009).
[8] W. Sakaguchi, S. Kajita, N. Ohno and M. Takagi, J. Nucl. Mater. **390-391**, 1149 (2009).
[9] S. Matsuo, H. Kurishita, H. Arakawa, T. Takeda, H. Kato et al., Mater. Sci. Eng. A, **492**, 475 (2008).
[10] W. Bohmeyer, A. Markin, D. Naujoks, B. Koch, G. Krenz, M. Baudach and G. Fussmann, J. Nucl. Mater. **363-365,** 127 (2007).
[11] F. Scotti and S. Kado, J. Nucl. Mater. **390-391**, 303 (2009).
[12] B. de Groot, R.S. Al, R. Engeln, W.J. Goedheer, O.G. Kruijt et al., Fusion Eng. Design **82**, 1861 (2007).
[13] H.J. Van Eck, W.R. Koppers, G.J. van Rooij, W.J. Goedheer, B. De Groot et al., Fusion Eng. Design **82**, 1878 (2007).